TIME-SERIES ANALYSIS OF REMOTELY-SENSED SEAWIFS CHLOROPHYLL IN RIVER-INFLUENCED COASTAL REGIONS

James G. Acker[1], Erin McMahon[2], Suhung Shen[3], Thomas Hearty[1] and Nancy Casey[4]

1. Goddard Earth Sciences Data and Information Services Center /Wyle IS, Greenbelt, Maryland, USA; jim.acker(at)nasa.gov, thomas.j.hearty(at)nasa.gov
2. Columbia University, New York, New York, USA
3. Goddard Earth Sciences Data and Information Services Center / George Mason University, Greenbelt, Maryland, USA; suhung.shen(at)nasa.gov
4. Science Systems and Applications Inc., Lanham, MD, USA; nancy_casey(at)ssaihq.com

ABSTRACT

The availability of a nearly-continuous record of remotely-sensed chlorophyll *a* data (chl *a*) from the Sea-viewing Wide Field-of-view Sensor (SeaWiFS) mission, now longer than ten years, enables examination of time-series trends for multiple global locations. Innovative data analysis technology available on the World Wide Web facilitates such analyses. In coastal regions influenced by river outflows, chl *a* is not always indicative of actual trends in phytoplankton chlorophyll due to the interference of coloured dissolved organic matter and suspended sediments; significant chl *a* time-series trends for coastal regions influenced by river outflows may nonetheless be indicative of important alterations of the hydrologic and coastal environment. Chl *a* time-series analysis of nine marine regions influenced by river outflows demonstrates the simplicity and usefulness of this technique. The analyses indicate that coastal time-series are significantly influenced by unusual flood events. Major river systems in regions with relatively low human impact did not exhibit significant trends. Most river systems with demonstrated human impact exhibited significant negative trends, with the noteworthy exception of the Pearl River in China, which has a positive trend.

INTRODUCTION

Large river systems respond to natural and anthropogenic changes in the regional watershed that provides their source of water. River outflow in coastal regions influences the coastal marine environment in several ways through the delivery of fresh water, nutrients, dissolved organic matter, and suspended sediments. Monitoring of trends in such constituents in coastal regions influenced by river outflow can thus indicate or identify alteration of the regional environment, both inland and along the coast.

Remotely-sensed chlorophyll *a* (chl *a*) from satellite sensors provides a method to examine trends in the coastal environment without the necessity of *in situ* sampling. Because chl *a* data in coastal regions essentially constitutes an indicator of the ambient ocean optical environment, identification of trends in this remotely-sensed variable can be potentially linked to terrestrial and human interactions in the river watershed (1,2). In order for such trends to be valid, the long-term accuracy of the data, by means of sensor calibration and ongoing data validation, must be reliable. It should be noted, however, that even though long-term accuracy of the chl *a* data parameter has been maintained, in coastal waters remotely-sensed chl *a* is a less accurate indicator of actual chlorophyll concentrations than in the open ocean due to increased turbidity (primarily coloured dissolved organic matter (CDOM) and suspended sediments) in coastal waters.

Although human actions will affect the entire ocean through long-term processes, rivers are frequently sensitive indicators of human activities. Numerous studies show that anthropogenic factors affect river flow as well as the nutrient and sediment supply, which in turn affects composition of species and ecosystem elements such as water and nutrient cycling (3,4). Rural

inputs, such as deforestation and agricultural production (5); and urban inputs, such as sewage systems and vehicular exhaust (6) cause increases in nutrients in the river. In addition, climate change can be related to changes in river patterns and nutrient loads (7,8). Increases in nutrient loading can threaten the ecological conditions in coastal zones surrounding the rivers through increased phytoplankton productivity, leading to eutrophication, hypoxia (low dissolved oxygen in bottom waters), and anoxia (zero dissolved oxygen in bottom waters) (9,10).

The Sea-viewing Wide Field-of-view Sensor (SeaWiFS) provides a nearly continuous, consistent and reliably-calibrated record of remotely-sensed chl *a* now exceeding 10 years in duration. Maintenance of SeaWiFS calibration, which is necessary for the maintenance of consistent chl *a* retrievals, has been accomplished through a series of monthly lunar calibration maneuvers that utilize the lunar radiance as a constant radiance source (11). Ongoing data validation efforts using research cruise data and data from moored optical sensors are also utilized to maintain consistent chl *a* retrievals.

Analysis of SeaWiFS data has shown a 4% global increase in chlorophyll from 1997 to 2003 with most of the increases occurring in the coastal zones (12). This study represents an initial systematic examination of different oceanic river outflow regions across the globe from 1998 to 2007.

As Earth remote-sensing data becomes increasingly accurate and spans longer continuous periods, analysis of coastal zone trends there is a greater need for easy access to this data for both scientists and interested citizens. The GES DISC Interactive Online Visualization And aNalysis Infrastructure (Giovanni) allows data acquisition and application of basic analytical functions using only a Web browser (13). By eliminating the barriers between data access and scientific inquiry, Giovanni can enable further research into coastal ocean trends and related datasets such as precipitation, wind, and atmospheric conditions. The usefulness of Giovanni to examine various aspects of the coastal zone has already been described (14).

Through its simplicity of use, Giovanni can provide the first step for scientific analysis of remotely-sensed chl *a* data. Several studies have used Giovanni to map chl *a* in regional studies, such as the Red Sea (15) the Chesapeake Bay (16) and seasonal variations in the northern South China Sea (17). By demonstrating the ease of chl *a* time-series analysis near river outflows, research to determine the causative factors involved with coastal chl *a* trends may be inspired, as well as more detailed research utilizing both remote sensing and *in situ* data. Such research can be useful both for coastal zone monitoring and also to improve understanding of the relationship between remotely-sensed chl *a* and *in situ* chlorophyll measurements in optically complex coastal waters.

River outflow influence on coastal waters

Rivers integrate environmental change factors, both natural and anthropogenic, over their entire watershed, giving insight into the changes occurring on the land. The regional climate, hydrology and climate changes within the watershed determine the seasonality, size, and outflow of the river. Topography plays an important role in the discharge and the type of sediment transported.

Humans can affect chlorophyll concentrations in the outflow region in two ways: via higher nutrient loading, particularly nitrogen and phosphorous, or by influencing the mean flow and sediment load. Increases in nutrients will commonly lead to increased phytoplankton productivity and thus an increase in remotely-sensed chl *a*.

Direct nutrient loading usually occurs due to land-use changes. Increases in nitrogen-rich fertilizer, phosphorous-rich sewage from urban waste, and run-off due to land-use change and deforestation are a few examples of direct nutrient loading. It is often hard to fully characterize these anthropogenic factors and even harder to quantify their effects.

Indirect nutrient loading is a result of changes in discharge and sediments, which carry nutrients. Discharge and sediment load provide insight into the nutrients entering the ocean from the river, especially through trends over time. In most cases, water discharge and sediment load exhibit a strong correlation. However, human-built reservoirs can skew this correlation. Reservoir dams can

block sediment transport and restrict discharge, causing decreases in nutrient delivery to the ocean.

Our study focuses on examining river outflow trends for significance and outlining some watershed alterations that may be related to these trends. We present the time-series results in conjunction with brief general descriptions of each river and river outflow region. This information outlines average discharge and sediment load, seasonality, and any human interference through dams. These are some of the primary factors that can lead to observable significant trends in coastal waters influenced by river systems.

METHODS

SeaWiFS global Level 3 monthly data products are acquired as they are generated by the NASA Ocean Biology Processing Group (OBPG) and ingested into the Giovanni system. SeaWiFS Level 3 data products are binned and averaged to global 9 × 9 km^2 resolution on an equal-area grid. Giovanni allows averaging of the mapped 0.083° × 0.083° grid values in any user-selected region. Average monthly chl *a* time-series are generated over the user-selected time period by generating the average chl *a* value for the selected region and then plotting each consecutive average value. Giovanni generates the arithmetic mean of the data values within the selected region.

In this study, Giovanni was employed to generated chl *a* time-series for nine distinct river outflow systems (The Mississippi River has both a western and eastern time-series due to the strong influence of a western-flowing coastal current). Figure 1 shows the selected areas chosen. Table 1 provides the corner coordinates for each region. Each area is a 0.5° × 0.5° region as close as possible to the river mouth, but possessing an average chl *a* concentration over the entire time-series not exceeding 1 mg/m^3. This concentration range was selected to reduce the influence of turbidity and CDOM, although their influence cannot be ruled out, particularly during high flow regimes, due to the known difficulty of discriminating CDOM from chl *a* in SeaWiFS data. In the case of large rivers, the area of ocean influenced by the river plume can be extensive; we utilized Giovanni to examine yearly averaged regional images to establish the apparent spatial extent of river-influenced waters. The Congo River-influenced region, for example, extends to at least 0° latitude from the river mouth location at 12° E latitude, approximately 1300 km; the Congo River study area was 1100 km from the river mouth. Because the lower concentration zones are situated near the boundary of the river-influenced region, alterations of flow regime or nutrient content would be expected to more significantly influence transitional regions than deeper in the river-influenced zone where conditions are less variable.

The Giovanni ASCII text output of time-series values was input into a MS Excel™ spreadsheet. Chl *a* time-series were generated over a nine-year time span. Linear regression was then applied to these complete monthly datasets using the least-squares linear fit method. This methodology is a simple way to perform trend analysis despite the potential sensitivity of the computational method to outliers. Significance of the linear model was determined by a 95% confidence interval ($p < .05$) using ANOVA analysis (18). The significance of the overall trend (and whether it was linear) was evaluated using the *f*-test. The r^2-value (coefficient of determination) was used to indicate how well the regression line fitted the actual data. In addition, we created plots of the yearly average of monthly chl *a* anomalies to mirror the 2005 study of global trends in chl *a* concentrations (12). These trends were calculated by 1) subtracting the average mean monthly value from each month which created monthly anomalies, 2) creating yearly anomalies by averaging the monthly anomalies for each year, and 3) applying regression analysis (Figure 15).

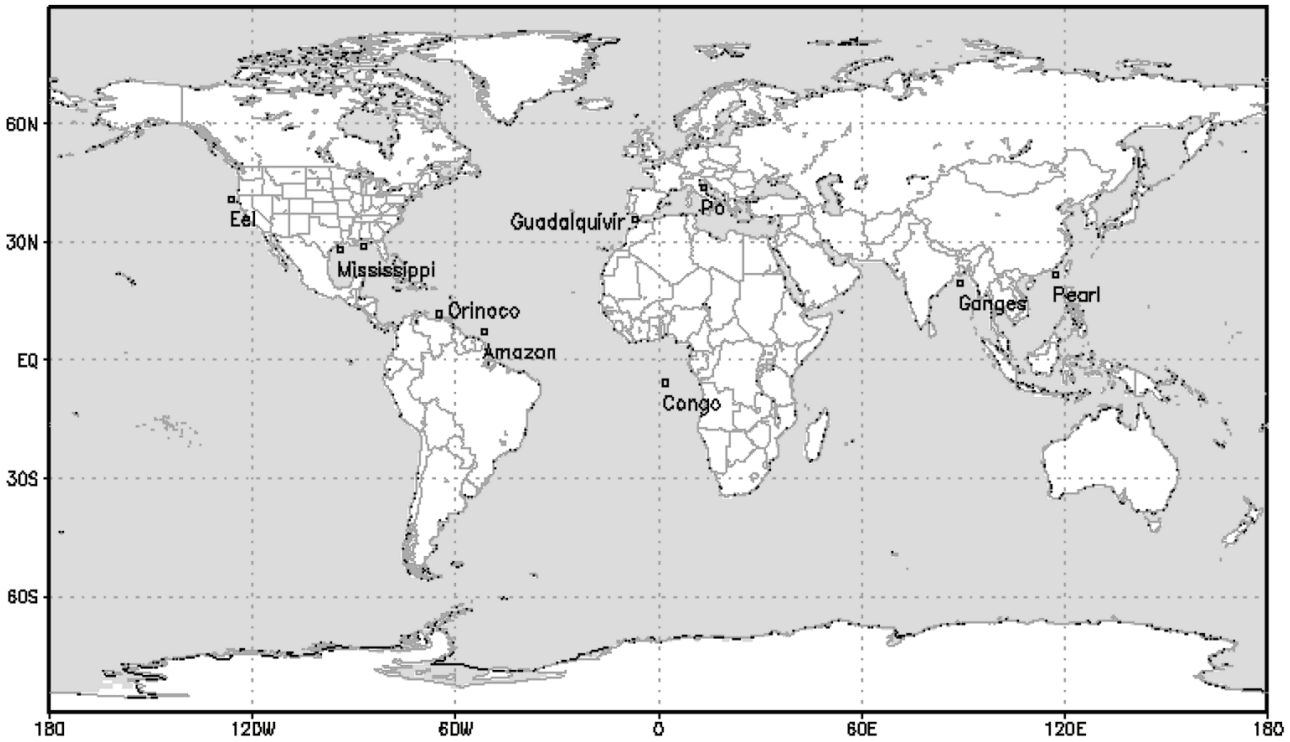

Figure 1: Map of the nine river outflows that were evaluated for this study.

Table 1: Latitude-longitude corner coordinates (in digital format) for the ten river-influenced 0.5° x 0.5° regions for which chl a time-series were generated.

RIVER SYSTEM	North	South	West	East
Amazon	8.0	7.5	-51.0	-50.5
Congo	-5.0	-5.5	2.0	2.5
Eel	41.5	41.0	-125.9	-125.4
Ganges	20.3	19.8	89.4	89.9
Guadalquivir	36.5	36.0	-6.8	-6.3
Mississippi (East)	29.6	29.1	-86.75	-86.25
Mississippi (West)	28.75	28.25	-94.0	-93.5
Orinoco	12.5	12.0	-64.8	-64.3
Pearl	22.5	22.0	117.5	118.0
Po	44.5	44.0	13.5	14.0

RESULTS

The results of each time-series analysis are presented subsequently. A brief description of the river system and potential influential factors in the watershed is presented with each time-series plot and statistical summary.

Amazon River

Physical description:
The Amazon River, which contributes approximately one-fifth of the total world river flow to the oceans, has an average discharge rate of 219,000 m^3/s. It encompasses a watershed basin of 6,915,000 km^2, which is the largest drainage basin in the world. As a tropical river, the Amazon is influenced by dry and rainy seasons. In this large basin, not all of the tributaries have the same seasonal flow, so the Amazon's seasonal peaks are produced by more than one river. The Amazon transports and deposits around 1200 million tons of sediment/year (19,20). Although there are few dams currently interrupting the Amazon's flow, a plan for two new hydroelectric dams was approved recently.

Time-series trend analysis:
The Amazon River has a slightly decreasing trend, but it is not significant. The yearly anomaly data also has a decreasing trend. The approximate distance of the time-series study area from the river outlet is 850 km.

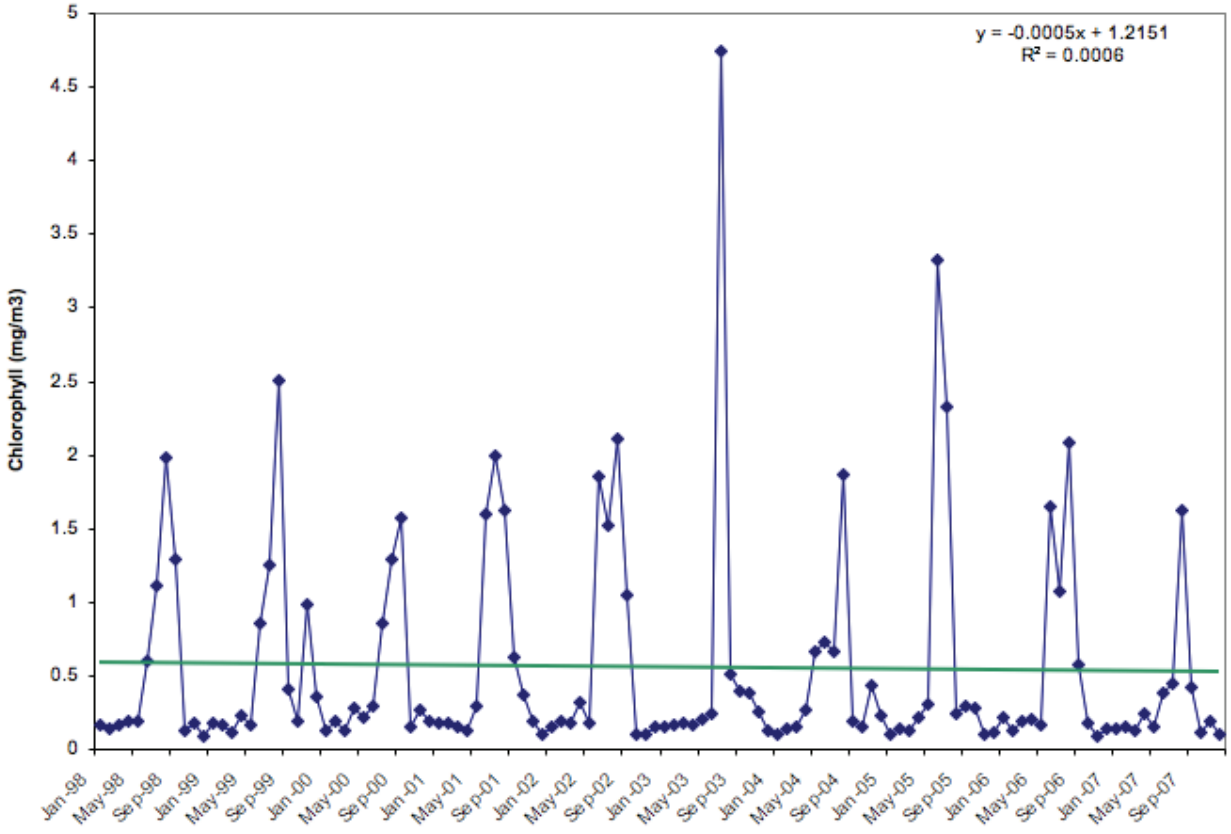

Figure 2: Time-series of SeaWiFS chl a for the Amazon River study area.

Congo River

Physical Description:
With the second-largest river outflow rate next to the Amazon, the Congo River has an average discharge rate of 41,800 m^3/s. Its watershed is slightly larger than the Mississippi at 3,680,000 km^2. It has a fairly stable flow with some seasonality. The Congo deposits around 30-40 million tons of sediments/year, which is mostly fine-grained (19,21). Because the sediments are mostly fine-grained and there is little human influence along the Congo, the sediment discharge is unusually low compared to other rivers. The Congo River currently has two large dams, Inga 1 and Inga 2. However, both are working at half their capacity.

Time-series trend analysis:
The Congo River shows a decreasing chl *a* concentration in the monthly and yearly anomaly data. Our study area was far from the coastline to avoid the $1mg/m^3$ chl *a* concentration values. This decreasing trend corresponds with the results presented in (12) which showed a few small areas with significant decreasing trends. However, the trend in our study region was not significant. The approximate distance of the time-series study area from the river outlet is 1100 km.

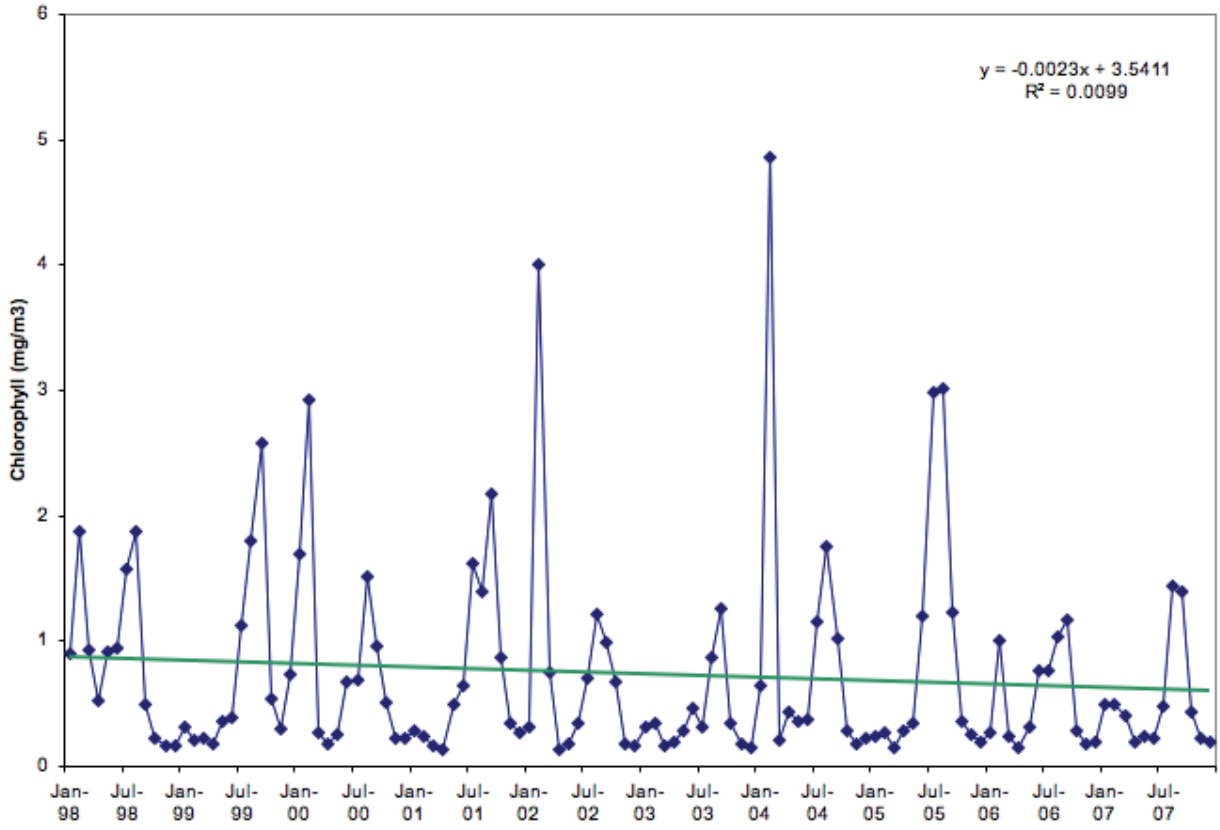

Figure 3: Time-series of SeaWiFS chl a for the Congo River study area.

Orinoco River

Physical Description:
Situated near the Caribbean Ocean, the waters from the Orinoco flow right into the warm Caribbean Sea near the Equator. It has an average discharge of 33,000 m^3/s. It occupies most of Venezuela with a watershed size of 880,000 km^2. For this tropical river, the two seasonal highs occur in May-June and November. The lows occur in March-April and August-September. The sediment output is about 150 million tons/year (19,22). In comparison to other temperate rivers such as the Mississippi, Ganges, and Pearl, the Orinoco has a low sediment yield. There are few dams, but the Volcan dam is the largest on the Orinoco River.

Time-series trend analysis:
The Orinoco shows a decreasing trend in the chl *a* time-series, but it was not significant. The approximate distance of the study area to the river outlet is 700 km.

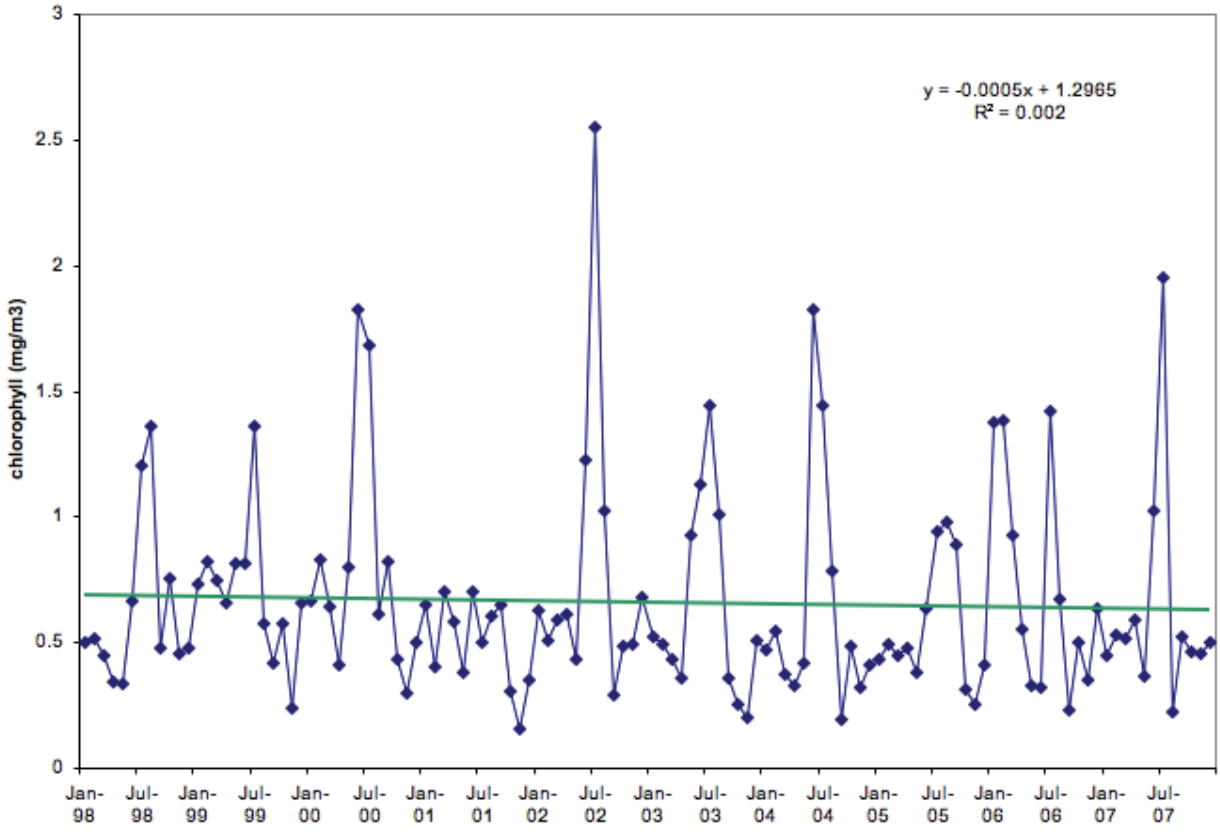

Figure 4: Time-series of SeaWiFS chl a for the Orinoco River study area.

Mississippi River

Physical Description:
Although it is likely the most well known of North American rivers, the Mississippi River is not the longest river in North America. However, it has the highest average discharge of 12,743 m^3/s. Its watershed basin spans 2,981,076 km2 with an annual sediment discharge to the Gulf Stream of around 210-230 million tons/year (19,24). The prevalence of farms in the watershed and their use of chemical fertilizers to improve agricultural productivity have led to unusually high sediment and nutrient discharges. According to the USGS, this discharge contains approximately 1,340,000 tons of nitrogen/year and 112,000 tons of phosphorous/year (25). As a temperate river, the Mississippi River experiences spikes in discharge during the spring snowmelt period in the northern watershed. During this time, high nutrient loading can occur. Due to these high nutrient loads, excessive phytoplankton growth causes hypoxic and anoxic conditions in the benthos at the mouth of the delta and in the coastal northern Gulf of Mexico. This is commonly referred to as the Mississippi River "dead zone". The Upper Mississippi has 29 locks and dams while the lower Mississippi has various wing dams and levees.

Time-series trend analysis:
The western section shows a larger decrease and a larger significance value than the eastern plot. Because the Mississippi River outflow tends to be transported west by the northern coastal current, the western section shows a more direct influence of the Mississippi River outflow.

The Mississippi River eastern section shows a decrease in chl *a* that is significant. The yearly data anomaly data also shows a decreasing trend. The approximate distance of the study area to the river outlet is 300 km.

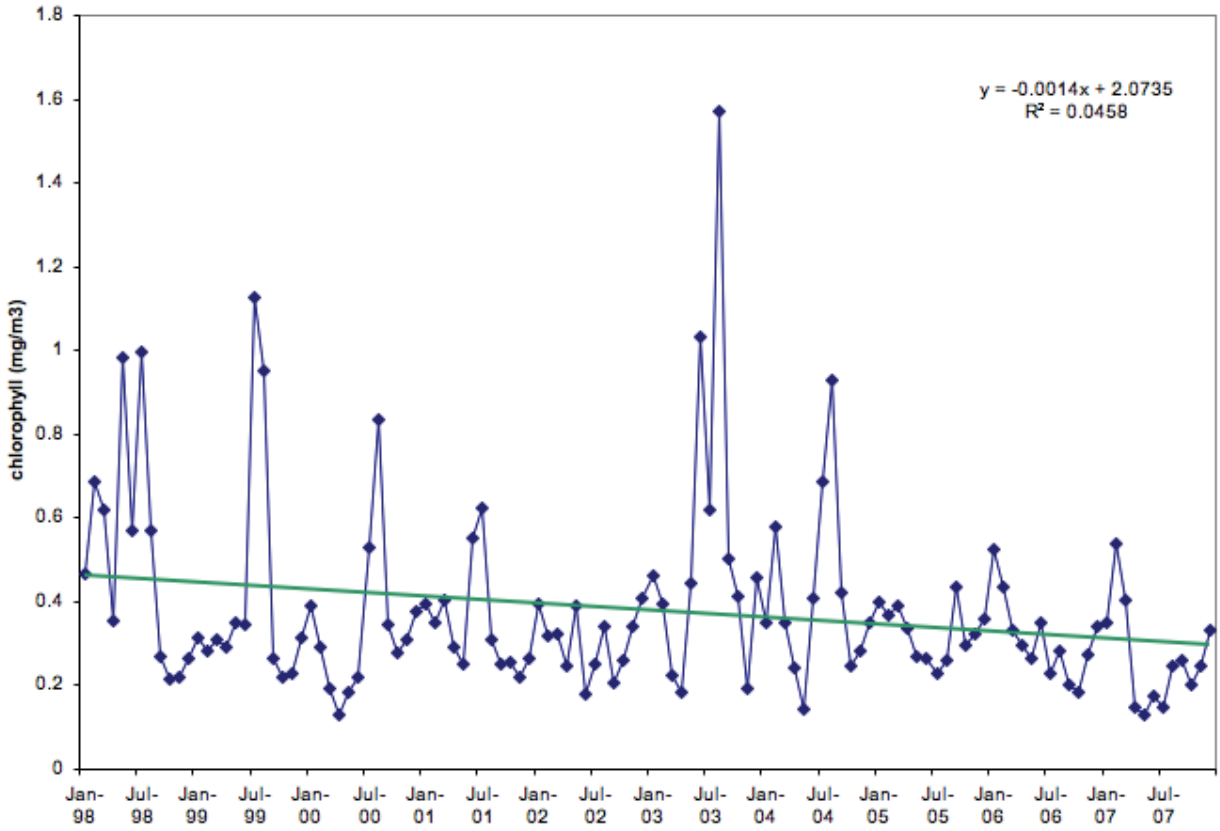

Figure 5: Time-series of SeaWiFS chl a for the Mississippi River – eastern section study area.

The Mississippi River western section data possess a larger decreasing trend than the eastern section, as does the yearly anomaly data. The Mississippi River western section time-series has

the largest significant trend (the largest *f*-value) of the time-series analyzed in this study. The distance of the study area to the river outlet is approximately 300 km.

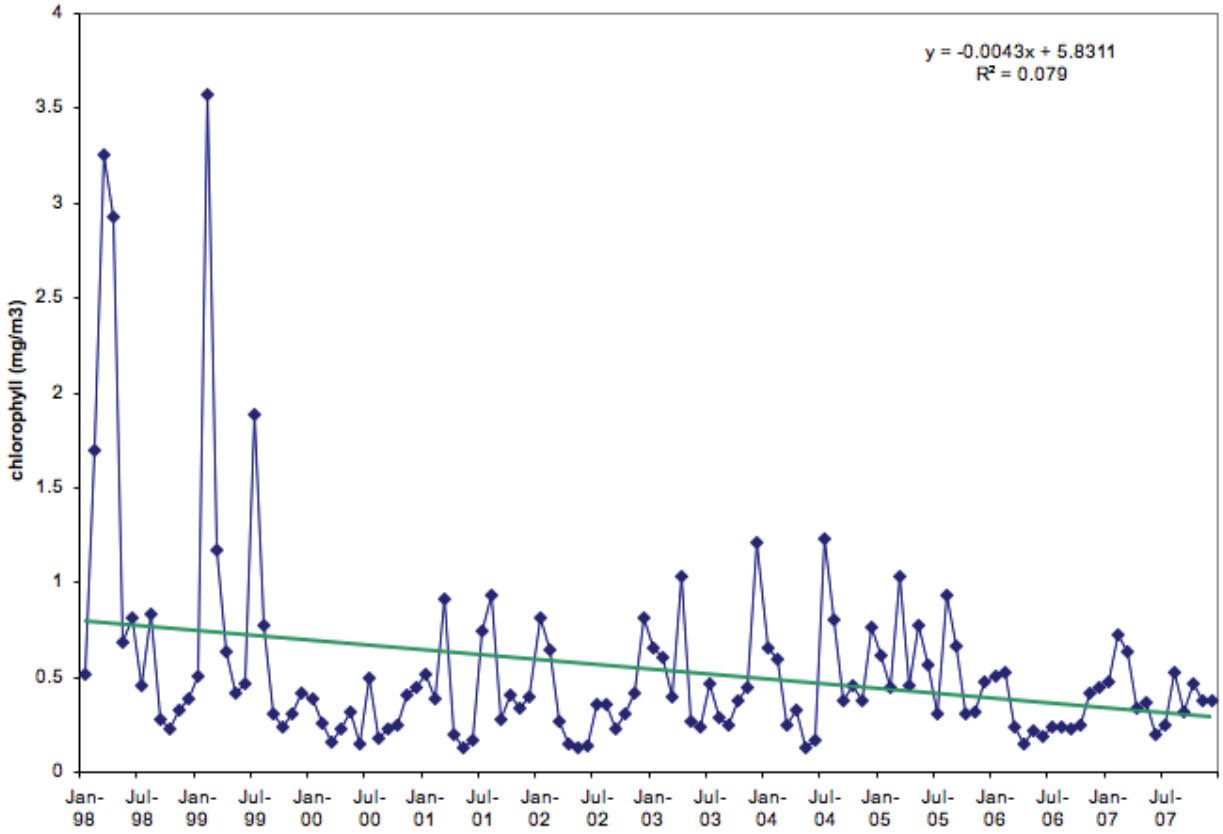

Figure 6: Time-series of SeaWiFS chl a for the Mississippi River – western section study area.

Pearl River

Physical Description:
The Pearl River has the second largest discharge volume in China with an average rate of 10,524 m^3/s. The drainage area is 453,700 km^2. It is highly seasonal with 80% of the discharge occurring during the wet season. It averages 70 million tons of sediment/year (19). The Pearl River has many small and large dams, including the second largest dam in Asia. But even with the decreasing water discharge due to dams and population increase, the Pearl River exhibits an increasing chl *a* trend.

Time-series trend analysis:
Unlike many of the other rivers, the Pearl River shows an increasing chl *a* trend in both the monthly time-series and the yearly anomaly. It is very close to a significant value at .068. The approximate distance from the river outlet to the study area is 400 km.

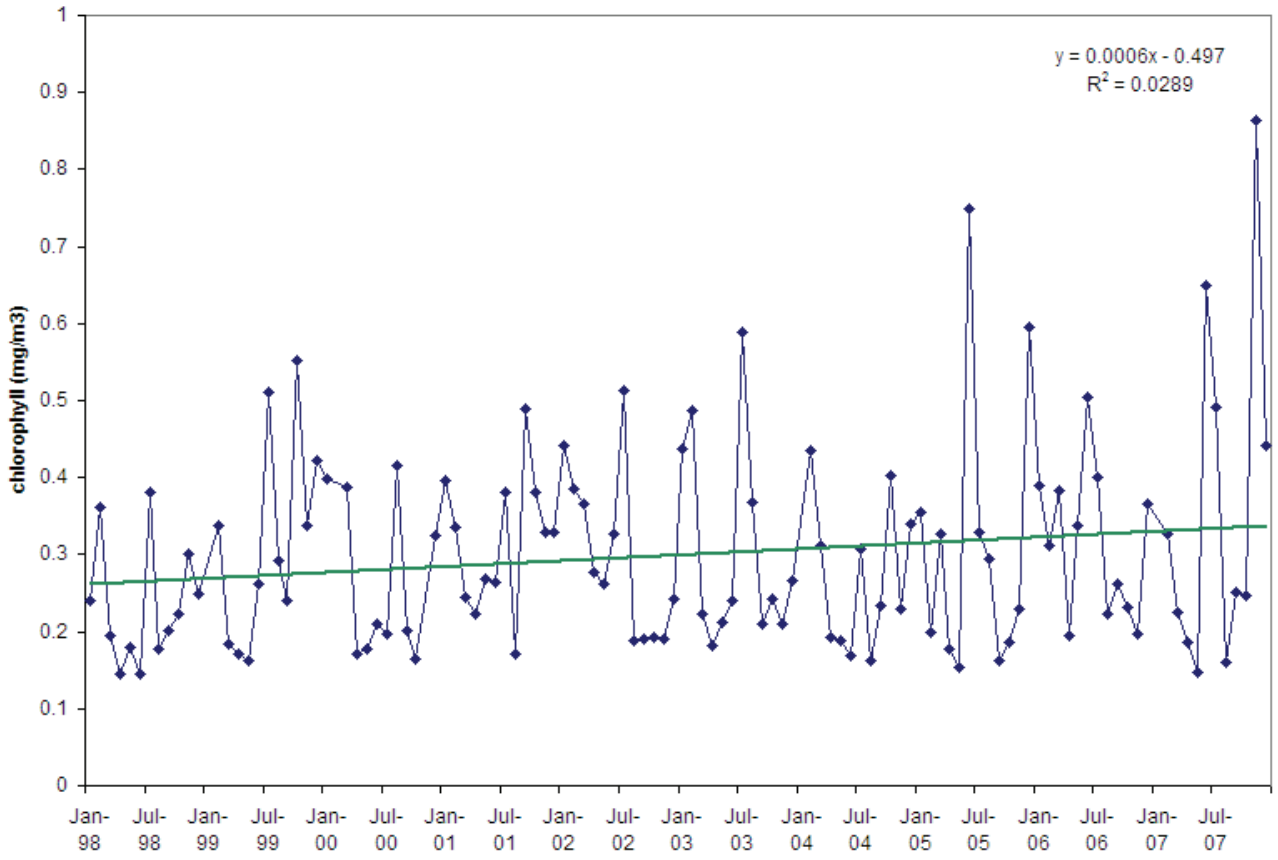

Figure 7. Time-series of SeaWiFS chl a data for the Pearl River study area.

Eel River

Physical Description:
Although a relatively small river in terms of discharge, due to topography, geology, and lack of human interference, the Eel River has the highest sediment yields per drainage area in the continuous United States. It spans an area of 9,542 km^2 with an average discharge of 200 m^3/s. The sediment yield is 14-16 million tons/year (19,26). As a temperate river, it is influenced by the freeze-thaw cycle. There are two dams on the Eel River, one of which diverts some of the Eel's flow to the Russian River. Although there are two dams, the Eel River is mostly wild. Because the Eel River showed increasing chl *a* concentrations without a correlating discharge or nutrient increase, we also compared chl *a* trends in the Eel River outflow region between summer months (which correspond to low flow), and the winter months (which correspond to high flow).

Trend Analysis:
Unlike many of the other rivers, the Eel River shows a significant increasing chl *a* trend in the monthly and yearly anomaly data. The approximate distance from the river outlet to the study area is 150 km.

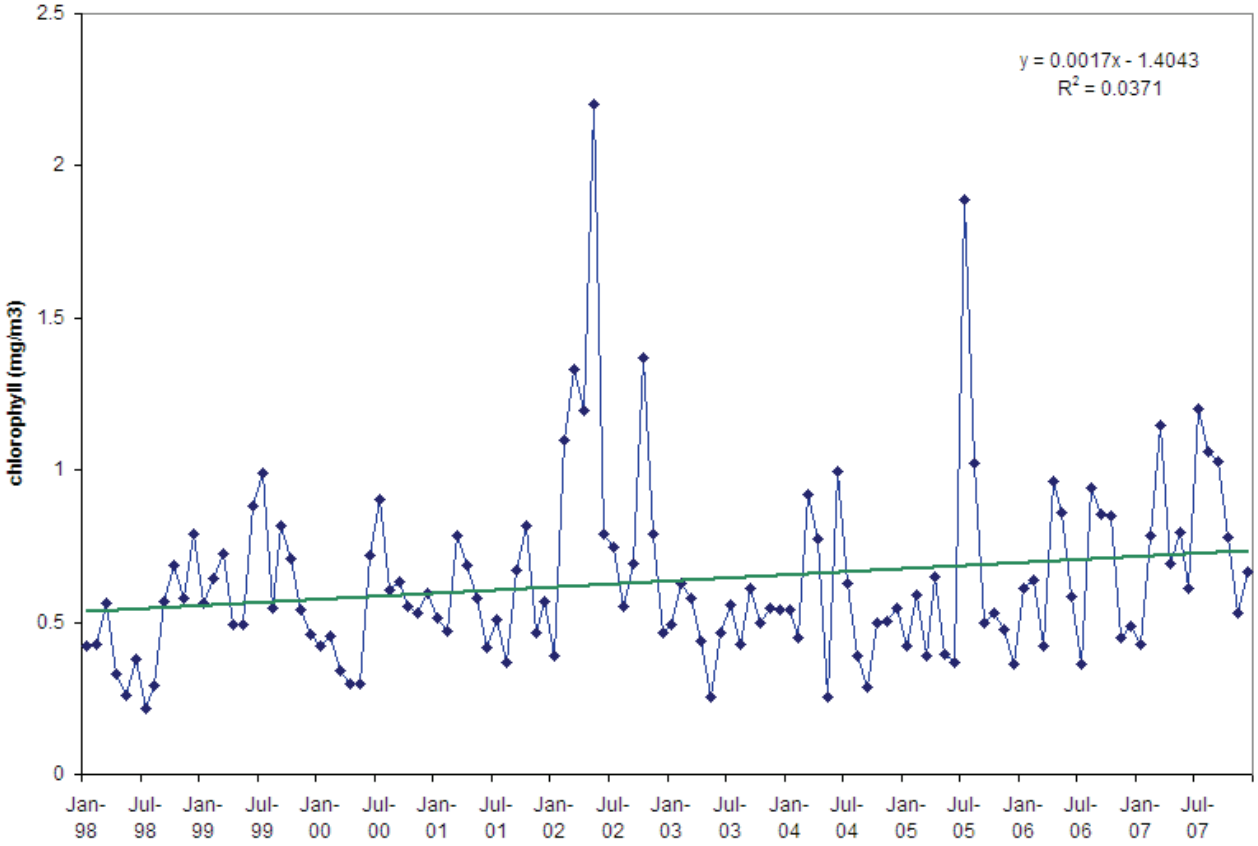

Figure 8: Time-series of SeaWiFS chl a data for the Eel River study area.

Seasonal Trend Analysis:
We divided the Eel River time-series data into two seasonal categories over the 10-year period: winter (November - April) and summer (May - October). The summer months indicated a close-to-significant increasing trend while the winter months showed no trend.

Table 2: Eel River SeaWiFS chl a time-series statistical summary for winter months (Nov-Apr).

Significance *f*	*f*-value	Slope	r^2	Average chl *a*
p = 0.29	1.125	0.0008	.0191	0.59 mg m^{-3}

Table 3: Eel River SeaWiFS chl a time-series statistical summary for summer months (May-October).

Significance *f*	*f*-value	Slope	r^2	Average chl *a*
p = 0.075	3.299	0.0024	.0536	0.68 mg m^{-3}

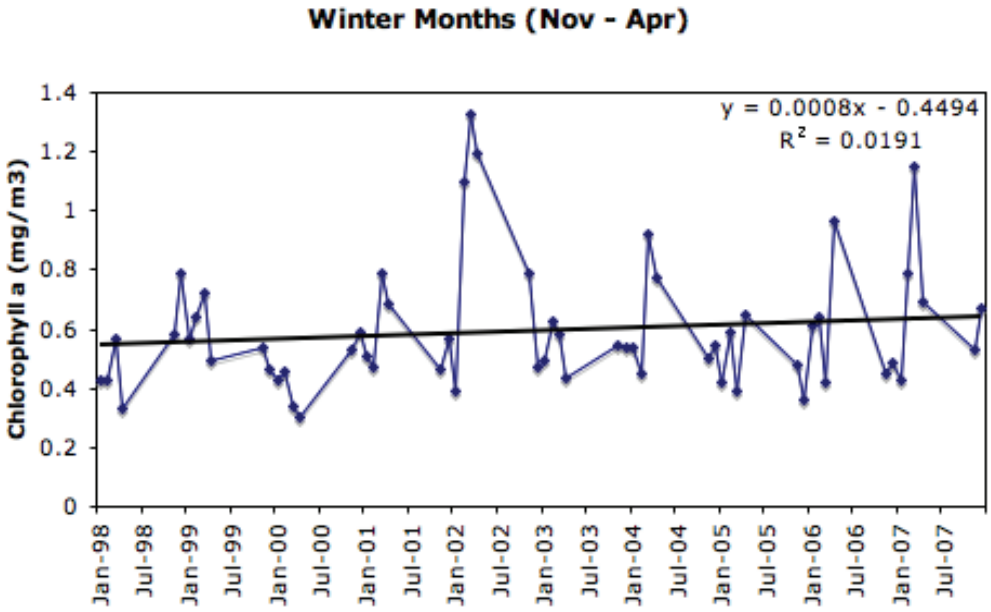

Figure 9: Time-series of SeaWiFS chl a data for the Eel River study area during winter months (November-April).

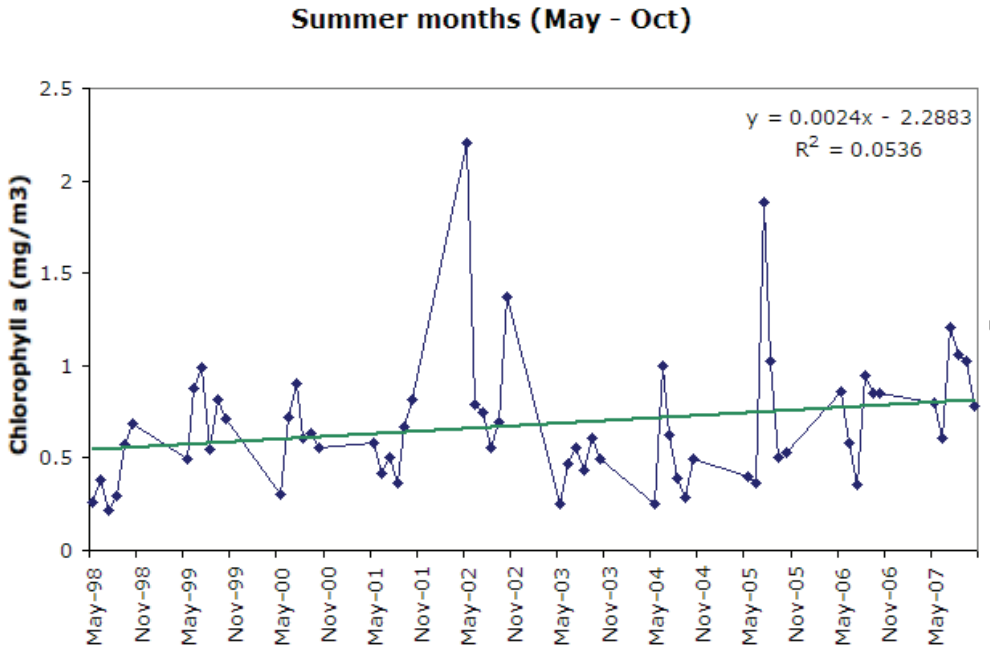

Figure 10: Time-series of SeaWiFS chl a data for the Eel River study area during summer months (May-October).

Ganges River

Physical Description:
The Ganges River has an average discharge of 12,015 m^3/s with a watershed basin of 907,000 km^2. The Ganges is also highly seasonal, following the flow of the monsoon season. It carries a sediment load close to 520 million tons/year - second in sediment discharge only to the Amazon (19,27). This high sediment discharge is due to the topography surrounding the Ganges watershed. The Himalayan Mountains lie to the north of the Ganges, and this high sediment load is carried downstream. The Ganges has 14 large dams, and India is interested in constructing 10 more dams to meet the needs of its high population (28).

Time-series trend analysis:
The Ganges shows a decreasing chl *a* trend across both datasets at a high significance value. The approximate distance of the river outlet to the study area is 275 km.

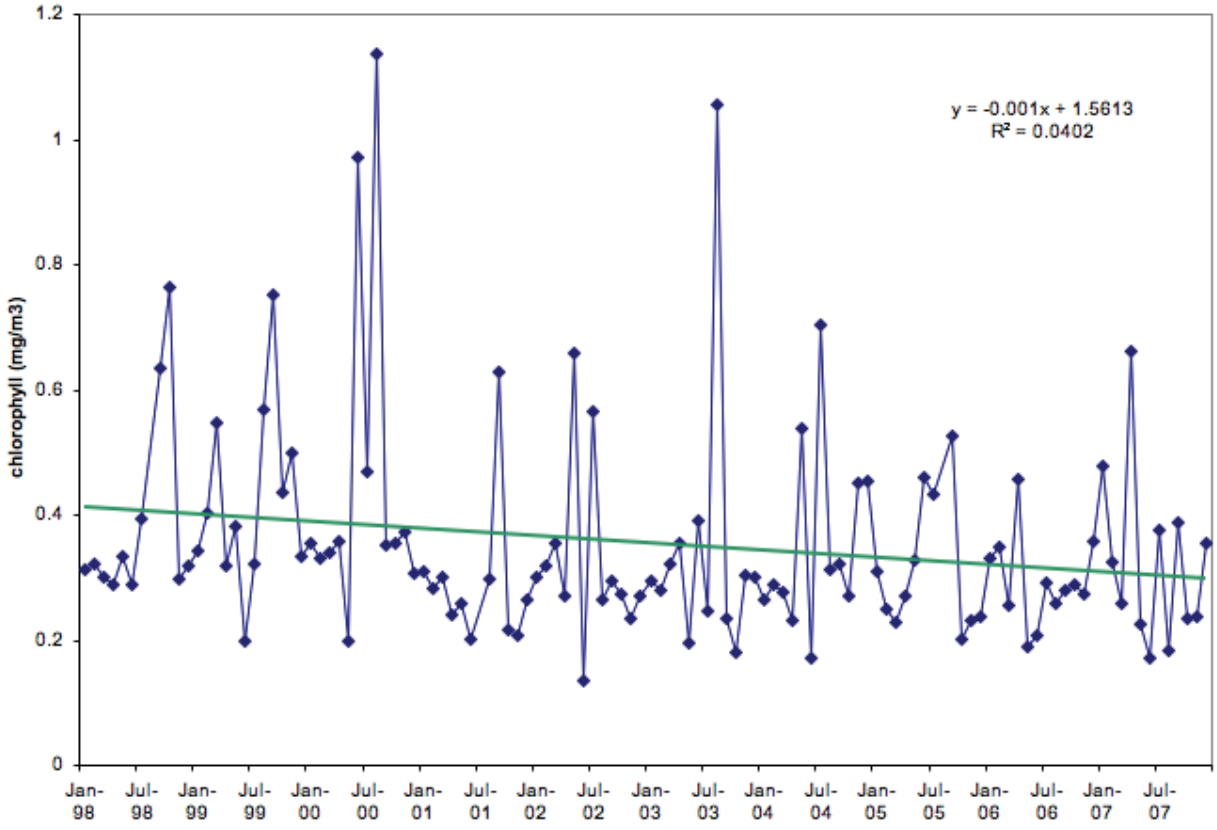

Figure 11: Time-series of SeaWiFS chl a data for the Ganges River study area.

Po River

Physical Description:
Beginning in the early Roman era, the Po River in Italy has been systematically diverted and influenced by human behavior. It is now a highly engineered river with numerous dams and levees that restrict its flow (29,30). The seasonality occurs during the June snow melt and the November cold frontal rain, but this is again restricted by human interventions. It has an average discharge of 1540 m^3/s, spanning a watershed of 70,091 km^2. The average sediment output is 15 million tons/year (29,30). A large spike in chl *a* concentrations, apparently related to a massive flooding event, occurred during October - December 2000.

Time-series trend analysis:
The Po River also has a decreasing trend in the SeaWiFS chl *a* monthly data. In addition, the trend becomes steadier following 2003 due to decreased water flow and human intervention in the Po. Even when the high chlorophyll value due to the rain event in October 2000 is excluded (Figure 13), the Po shows a decreasing trend with a close-to-significant value of .065.

The Po River shows a significant decreasing trend with the rain event of October-December 2000 included in the analysis. The approximate distance from the river outlet to the study area is 150 km.

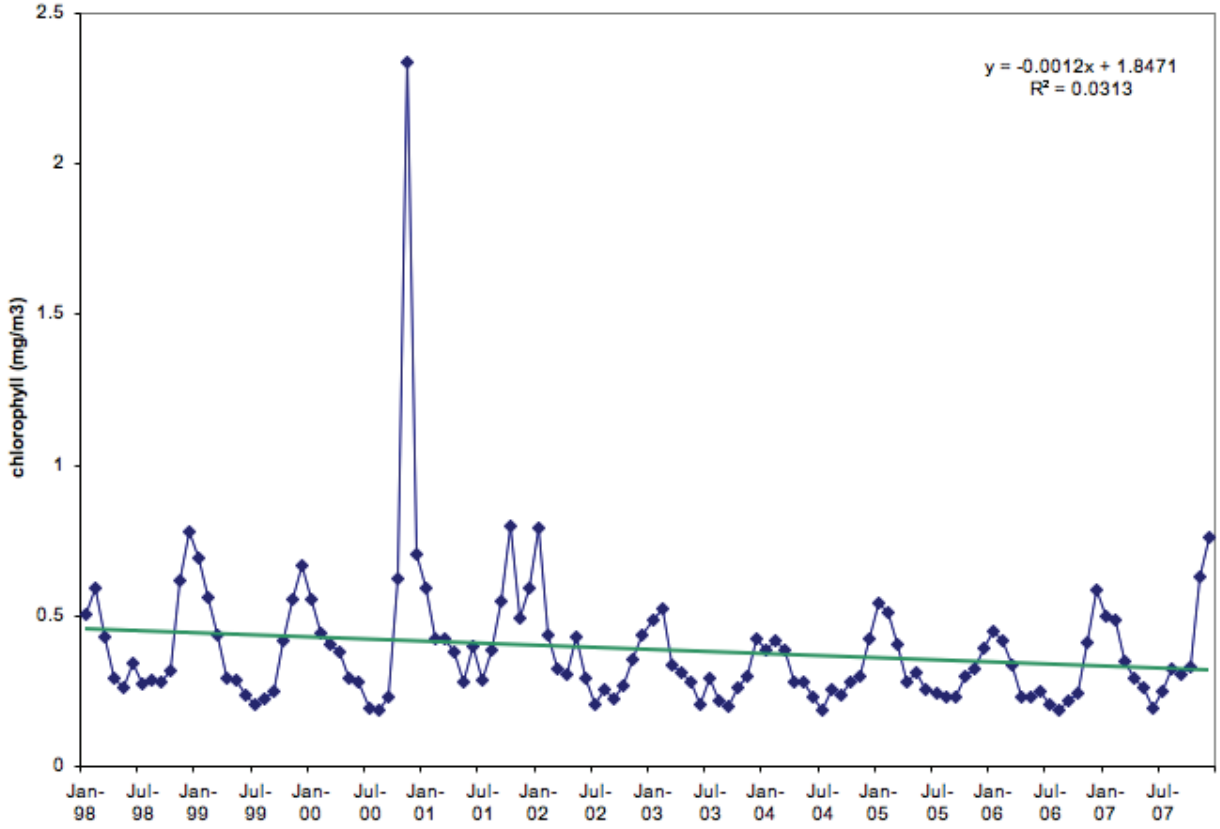

Figure 12: Time-series of SeaWiFS chl a data for the Po River study area.

After excluding the large spike in October - December 2000 heavy rain event, a decreasing trend persists that is very close to a significance level.

Table 4: Statistical summary of the Po River SeaWiFS chl a time-series analysis, excluding October-December 2000 data, for comparison to the values in Table 5.

Significance *f*	*f*-value	Slope	r^2	Average chl *a*
p = 0.065	3.45	-0.0007	.0295	0.36 mg m^{-3}

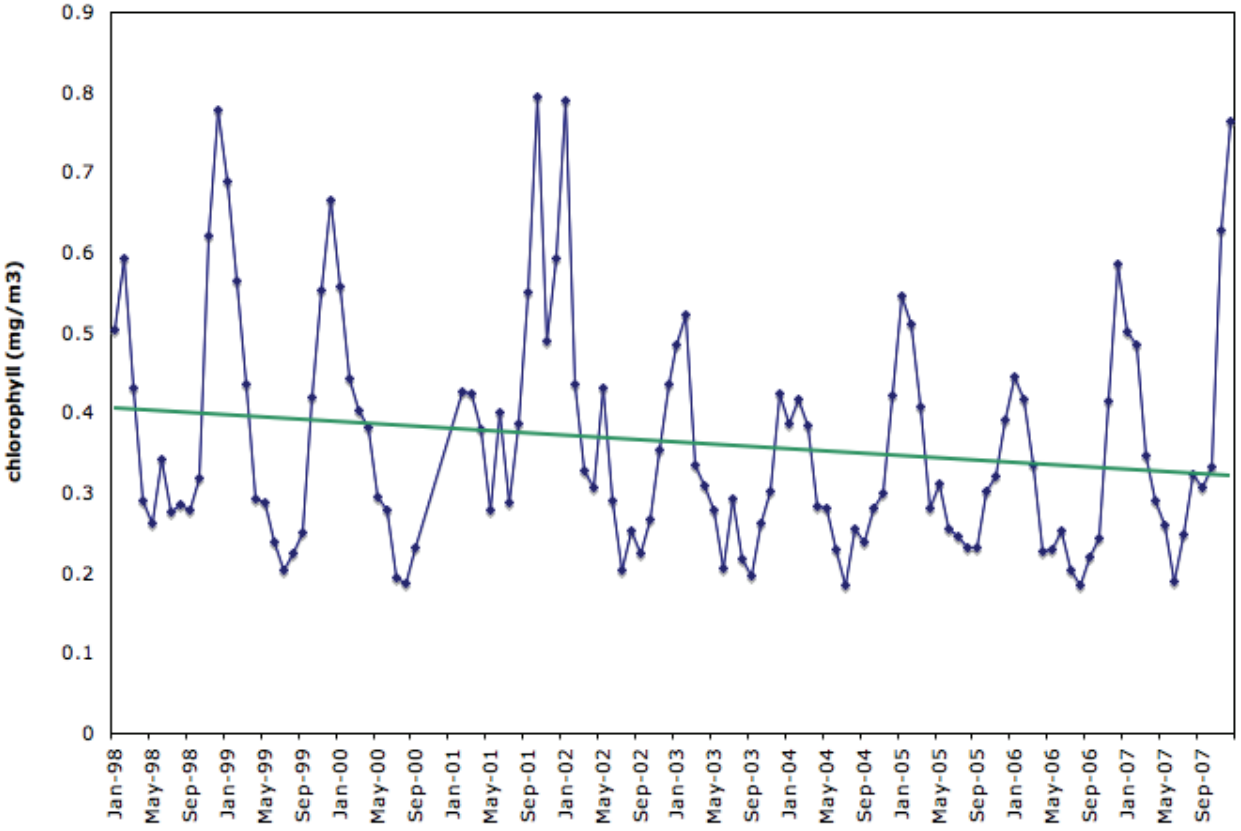

Figure 13: Time-series of SeaWiFS chl a data for the Po River study area, with data from October-December 2000 excluded.

Guadalquivir River

Physical Description:
Like the Po River, the Guadalquivir in Spain, another great river of Europe, has been influenced by human interaction. It has an average discharge of 164.3 m^3/s and watershed area of 56,978 km^2. Given the low discharge and the high human intervention through dams, the sediment yield is most likely very low for this river. It is still navigable until the town of Seville, but land use, dams, and water stress due to the high population density have decreased its water and sediment discharge rate, causing decreases in chlorophyll concentrations as well.

Time-series trend analysis:
The Guadalquivir River also has a decreasing trend in both datasets. It almost reaches a significance value at .07.

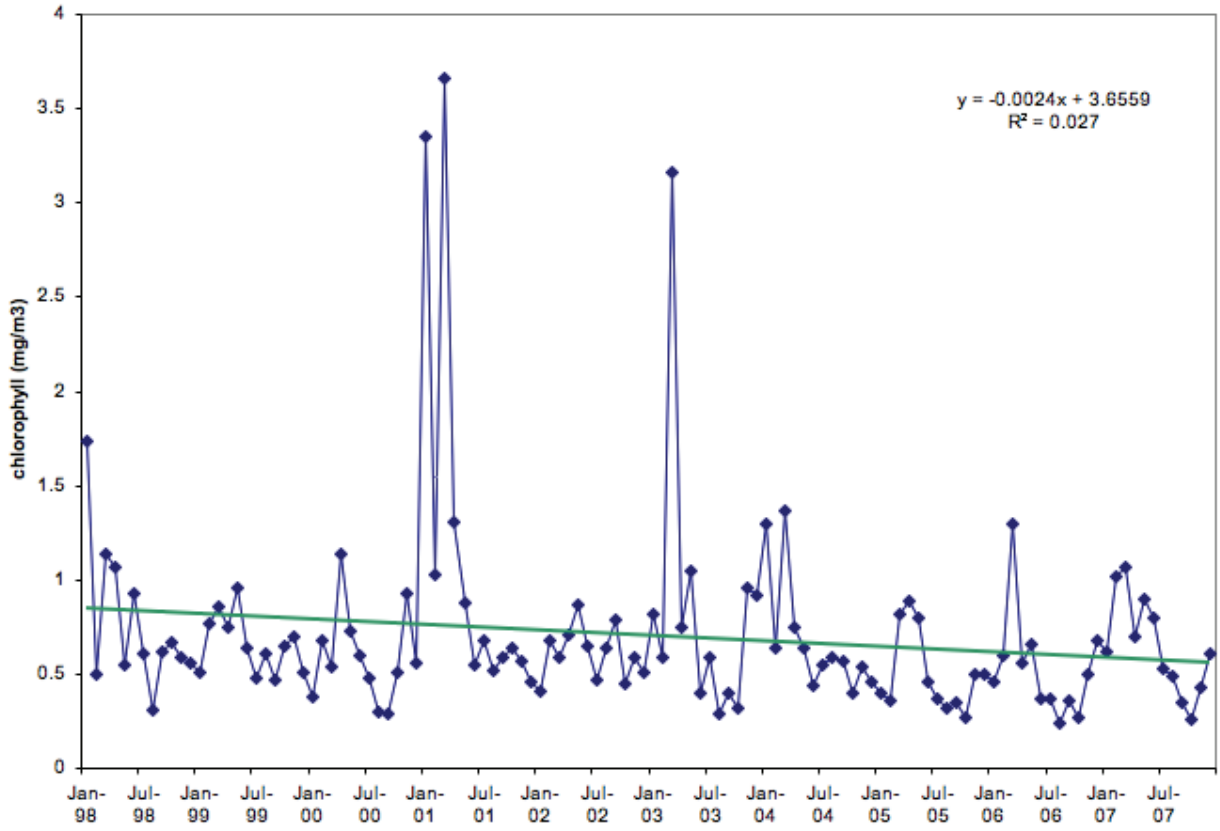

Figure 14: Time-series of SeaWiFS chl a data for the Guadalquivir River study area.

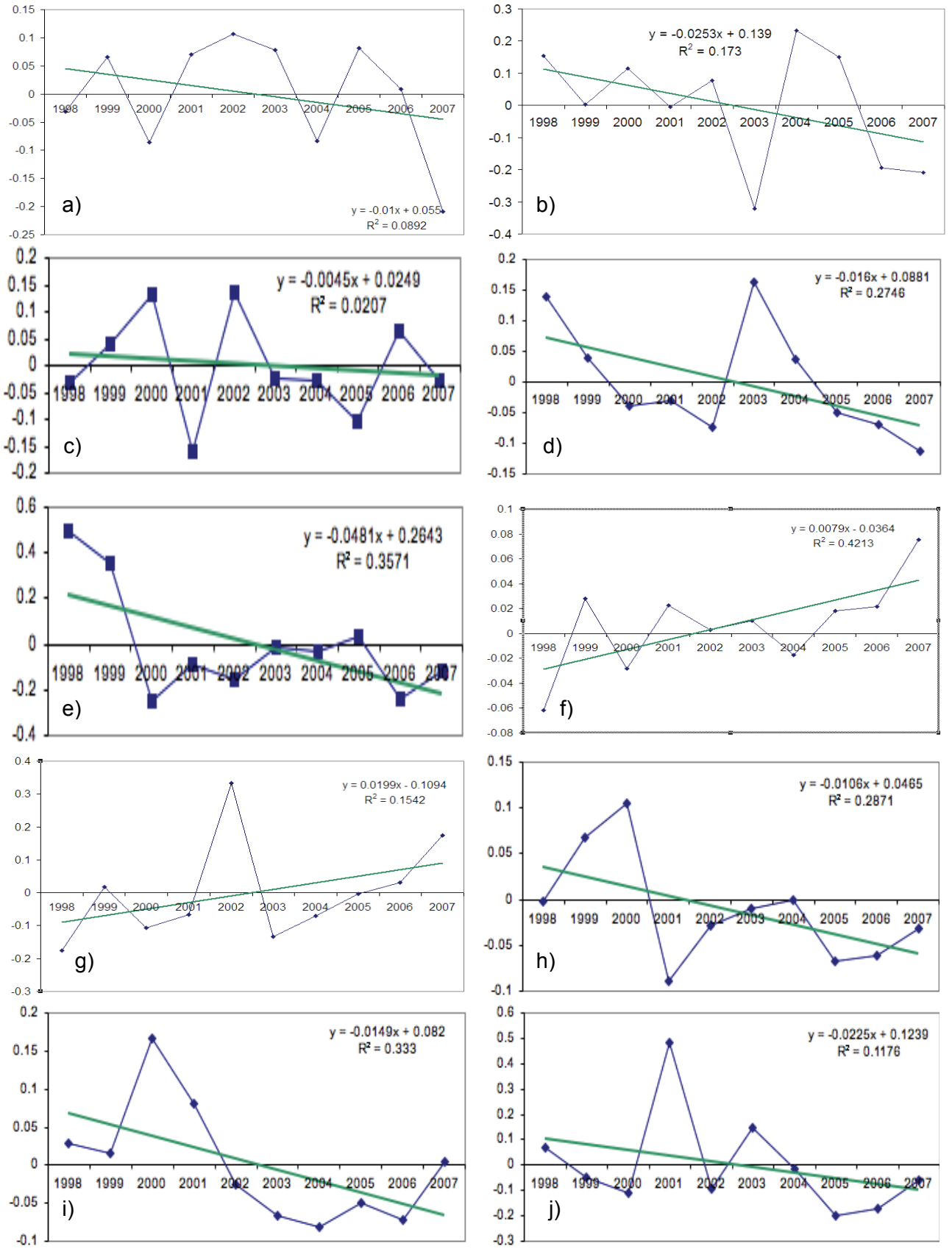

Figure 15: Time-series of annually-averaged monthly SeaWiFS chl a anomalies for the ten river outflow regions analyzed in this paper. a) Amazon River; b) Congo River; c) Orinoco River; d) Mississippi River eastern region; e) Mississippi River western region; f) Pearl River; g) Eel River; h) Ganges River; i) Po River; j) Guadalquivir River.

CONCLUSIONS

The following discussion presents an evaluation of the statistical methods used in the study, and discusses some of the influencing factors which are suggested as causative for the observed trends.

Table 5: Summary table of full time-series analysis parameters for the ten river outflow zones examined in this study. 'Distance' indicates the distance from the river outlet to the study area. A significance f value less than 0.05 indicates a significant trend at the 95% confidence level.

RIVER SYSTEM	Distance	Significance *f*	*f*-value	Slope	r^2	Average chl *a*
Amazon	850 km	p = 0.78	0.07	-0.0005	0.0006	0.55 mg m^{-3}
Congo	1100 km	p = 0.28	1.17	-0.0023	0.0099	0.728 mg m^{-3}
Eel *	150 km	p = 0.035	4.53	+0.0017	0.0371	0.64 mg m^{-3}
Ganges	275 km	p = 0.03	4.8	-0.001	0.0402	0.35 mg m^{-3}
Guadalquivir	65 km	p = 0.07	3.28	-0.0024	0.027	0.70 mg m^{-3}
Mississippi (East)	300 km	p = 0.0169	5.66	-0.0014	0.0458	0.38 mg m^{-3}
Mississippi (West)	300 km	p = 0.0018	10.12	-0.0043	0.079	0.54 mg m^{-3}
Orinoco	700 km	p = 0.63	0.23	-0.0005	0.002	0.66 mg m^{-3}
Pearl	400 km	p = 0.068	3.37	+0.0006	0.0289	0.30 mg m^{-3}
Po **	150 km	p = 0.053	3.8	-0.0012	0.0313	0.39 mg m^{-3}

* Includes all annual data.

** Includes October-December 2000 data.

Statistical Methods

One of the motivations for this study was to demonstrate the ease of using Giovanni data output for examination of time-series trends. It is relatively simple to extract the ASCII data output and place it in an MS Excel® spreadsheet, which allows utilization of the data plotting and analysis capabilities in this software package (including the statistical package that allowed generation of the significance f values). At the same time, any such analysis is constrained to the analysis capabilities of this software. The research demonstration did not intend to subject the data to more extensive statistical analysis. The ease of generating the data output from Giovanni makes it possible to analyze the data with other more advanced software packages.

One of the limitations of the MS Excel® software is the trend-related regressions that are provided. While it would be possible to fit the data to polynomial or logarithmic functions (as examples), these functions do not provide more information about the existence or robustness of a trend (applying a moving average is also possible and could yield additional insight). It was, however, recognized that the simple linear regression utilized would be sensitive to outliers in the time-series data. The low r^2 values indicate, as would be expected, that there is limited dependence of month-to-month chl *a* values in the outflow regions, and thus episodic events could influence the appearance of longer-term trend. Due to the influence of outliers on the simple linear regression, we also analyzed the data utilizing the robust linear regression function available for Matlab (31), which also shows the potential use of Giovanni output for more advanced statistical studies.

The results of this analysis are shown in Table 6, where the slopes of the simple linear regression trendlines are compare to the slopes of the robust linear regression trendlines. In general, the robust linear regression method results in a reduction of the slope (both positive and negative), particularly if the time-series contains a few exceptional events at the beginning or the end of the time-series. The influence of such events indicates the necessity for continuation of remotely-sensed ocean colour data sets to enable improved evaluation of long-term trends. A comparison of the slopes from the two regression methods is shown in Figure 16 for the Mississippi River west region, which exhibited one of the largest shifts in the value of the trend line slope.

Table 6: Comparison of trendline slopes generated by the simple linear regression and robust linear regression methods.

RIVER SYSTEM	Trendline slope: Simple linear regression	Trendline slope: Robust linear regression
Amazon	-0.0005	-0.0002
Congo	-0.0023	-0.0026
Eel	0.001	0.0014
Ganges	-0.0006	-0.0007
Guadalquivir	-0.0024	-0.0014
Mississippi (East)	-0.0029	-0.0011
Mississippi (West)	-0.0043	-0.0005
Orinoco	-0.0005	-0.0007
Pearl	0.0013	0.0005
Po	-0.0035	-0.0009

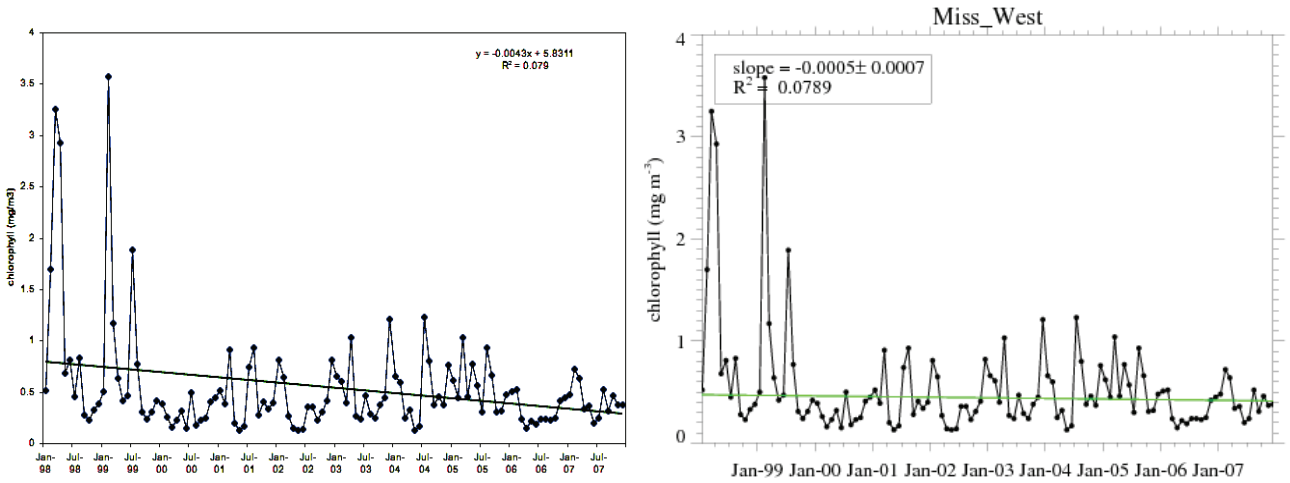

Figure 16: Comparison of the trendline slopes generated by the simple linear regression method (left) and robust linear regression method (right) for the Mississippi West region.

Amazon, Orinoco, and Congo Rivers

The three rivers without a significant chl *a* trend in the study area - the Amazon, Orinoco, and Congo - are close to the Equator in the Southern Hemisphere. The tropical dynamics that affect these rivers are different than the other rivers in our study. Unlike temperate climates, tropical rivers are not influenced by freeze-thaw cycles (32). Rather, seasonality is dependent on rainy-dry seasons, grounded in an increase or decrease in precipitation levels. The tropical dynamics might have some effect on why trends in these areas are not significant. However, the more likely cause is the dichotomy between 'developing' tropical regions and 'developed' temperate regions surrounding the rivers (32). The Orinoco, Amazon, and Congo are still, for the most part, unaffected by anthropogenic factors. Their watersheds are in developing countries with few (if any) dams causing disruption of the natural flow or water impoundment. Because human impacts provide the greatest environmental alteration and stress to river ecosystems, this lack of anthropogenic forcing is a likely reason for the lack of observed trend. Another factor may be in our study methodology. Each of these rivers has a substantial discharge, and hence a large plume influenced by sediment and nutrient discharge. To find an area in the average chl *a* range below 1 mg/m^3, which would exclude much of the interference from sediment discharge and nutrient-enhanced productivity, we were constrained to choose a sampling region significantly farther from the coastline than required

for the smaller rivers. This site selection criterion may have caused the observational plots to be more influenced by ocean dynamics than areas nearer to the coast.

Mississippi River

The Mississippi River shows the most significant decrease in chl *a* concentrations of the analyzed areas, yet this observation was influenced by high-discharge events occurring early in the time-series. Large volumes of nutrient-rich water have been correlated with satellite-derived and *in situ* chlorophyll concentrations off the Louisiana shelf (33,34). The latter study (34) demonstrated the relationship between chl *a* and nitrate loading with a lag time of one month, while (33) linked this to phosphorous, silicate, and other nutrients. Decreasing chl *a* concentrations could be a result of federal and state government efforts to reduce the anoxic and hypoxic benthic zone near the Mississippi River delta by decreasing nitrogen output to the river. Total annual loads from 2001 to 2005 show a 21% decrease in nitrogen loads from the average values from 1986-1996. However, there was a 12% increase in phosphorous loads over this same period (35). Because nitrogen tends to be the limiting nutrient in the Mississippi River system (with a ratio of 16:1 to phosphorous,) the decrease in nitrogen will decrease algal growth even with an increase in phosphorous. (36). But although chl *a* correlates well with nitrogen loading, chl *a* was not clearly correlated with the extent and frequency of hypoxia. The western plot resides in the hypoxic zone of the Mississippi outflow for 2007. Since 1998, the hypoxic zone, often referred to as the Gulf of Mexico “dead zone”, has been growing in size (34). Although hypoxia off the Louisiana coast has been linked to nutrient-enhanced productivity and hence chl *a,* the link is not a direct one (37). Accumulation of organic material from past years can affect hypoxia in subsequent years (38). In addition, wind speeds and direction also affect the stratification of waters, which is key to development of hypoxic conditions (33).

Pearl River

Although its average discharge has decreased due to dams and human adjustments (39) the Pearl River actually exhibits an increasing chl *a* concentration. The Pearl River Delta is one of the most productive agricultural areas in China and one of the most rapidly developing areas with increases in economic activity and population (40,41). These changes have led to increased agriculture, fish farming, and sewage effluents, and thus likely contribute to dramatic increases in nitrogen fluxes to the river. Historically, China has relied on organic fertilizer for crop production, which reduced the unused nitrogen in human and animal excreta to the environment. From 1949 -1995, there was a 100% increase in fertilizer use. In addition, the ratio of inorganic to organic fertilizer decreased by 60% (42). The shift to chemical fertilizer has caused an increase in nitrogen-loading to the environment and a decrease in nitrogen in excreta utilized by agriculture. With the decline of organic fertilizer and the increase in urban population, nitrogen-rich sewage outflow to the Pearl has increased. In addition to agriculture, land use changes have also increased runoff, causing more nutrient loading into the Pearl River (43).

Eel River

The Eel River of California provides an odd case due to the increasing values of chl *a* observed in our study area. There is no evidence to suggest increasing fertilizer use or other new sources of nutrients to the river system. In fact, U.S. Geological Survey discharge at the Scotia Station near the mouth of the Eel River shows a decreasing flow rate over time, suggesting less nutrient input from the river system (Figure 17). Seasonally, the Eel River has higher chl *a* concentrations during the summer months and an increasing chl *a* trend (Figure 17). In contrast, the winter months show lower chlorophyll concentrations and a minimal chl *a* trend (Figure 16). From the data at USGS Scotia River Discharge Station, we can see that the highest discharge occurs during the winter months rather than the summer months (Figure 18). This suggests that the perceived trend in the summer months is due to marine rather than riverine sources. In the summer months, the discharge is low and the influence of the river output will not extend as far into the coastal ocean. Rather, the marine environment has more influence on our study area during the summer months. There are numerous reasons why the marine environment might generate more phytoplankton chlorophyll, such as increased sea surface temperature leading to more pronounced stratification

or an increase in upwelling. This particular intriguing aspect of our study deserves more detailed examination with additional data sources.

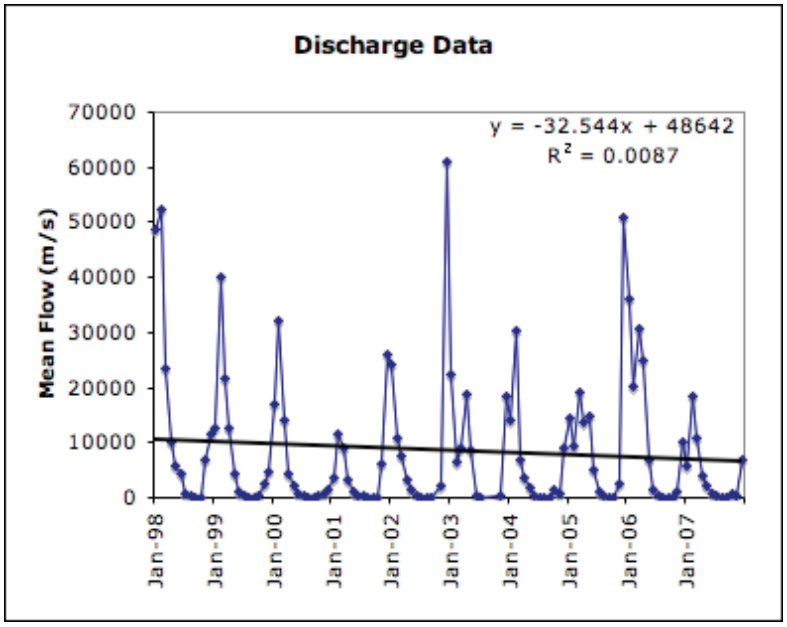

Figure 17: Monthly discharge data averaged from daily average flow rates at the USGS Scotia station near the Eel River mouth.

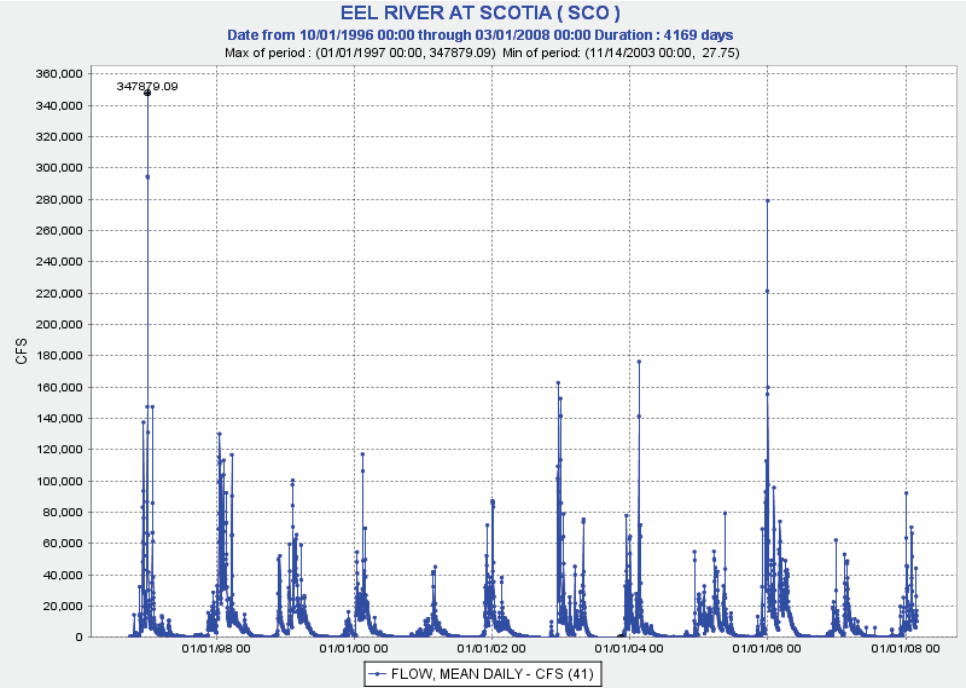

Figure 18: Daily mean flow data from the U.S. Geological Survey gauge station at Scotia, an area near the mouth of the Eel River. Data was plotted for the period October 1, 1996 to March 1, 2008 to include the 1998-2007 study period. (Data plot generated by the California Department of Water Resources California Data Exchange Center, http://leva.water.ca.gov/)

Ganges River

The Ganges has experienced a decrease in annual outflow with up to a 60% water loss due to diversion in the last 25 years (44). The decreasing discharge could be a result of new water stresses in the Ganges River Basin due to population increases and climate change. With rapid population increases, more water must be utilized for drinking and electricity-generation. As a re-

sponse to these pressures, many dams have been constructed along the Ganges. In 2004, the World Wide Fund for Nature identified the Ganges River (in its report 'Rivers at Risk') as one of the 20 most susceptible rivers. These water stress changes might already be appearing due to the number of large-scale dams (28). In addition, while climate change might also be increasing the discharge of the Ganges (45), human factors will likely increase demand on Ganges River water resources. Our data also shows a decreasing chl *a* trend. Decreasing flow may decrease the amount of nitrogen available for phytoplankton productivity in the Bay of Bengal. Therefore, the chl *a* trend is most plausibly related to decreasing discharge.

Po River

In October 2000, the Po River experienced a 100-year flood, which contributed a prolonged elevated discharge level from October 13, 2000 through December 4, 2000. Although the Po River has been almost 'tamed' by dams, the effects of the flood were drastic. Sustained discharge caused an influx of nutrients and sediments into the Po River (46). At the mouth of the river, the total suspended matter (TSM) decreased the light available to the phytoplankton. Therefore, the chl *a* concentration was not high at the river mouth. Farther south, the TSM decreased, allowing light to reach the phytoplankton below the surface. The light coupled with the high nutrient loads led to an intensive diatom bloom in the southern area with nutrient deficiency and oxygen saturation up to 200% near our sample plot (47). Our time series shows this increase in chlorophyll for the month of November 2000, exhibiting the diatom bloom and its associated chl *a* peak concentration.

Comparison to previous research

The results of our study, in which we observe a reduction of chl *a* concentrations over the time-series period in many of the river outflow zones, seem to be at odds with the observations of Gregg et al. (12). In this paper, a 4% increase in global chlorophyll concentrations was reported, with most of the increase occurring in the coastal zone. Gregg et al. indicate that most of the increase occurred in the following regions: the Patagonian Shelf, Bering Sea, eastern Pacific, southwest African, and Somalian coasts. Only one of these regions, southwest Africa, corresponds to one of our study regions, the Congo River outflow zone, and our study region may have been slightly further from the southwest African coast than the region where significant increasing trends were observed by Gregg et al. In fact, most of the regions we examined do not exhibit a significant trend in either direction in the Gregg et al. global compilation. One region, the Adriatic, exhibits a decreasing trend that may be compared to our results for the Po River, but our study region was located closer to the Po River mouth than the Adriatic Sea region which shows a decreasing trend. In the first attempt to utilize Giovanni's time-series capability to investigate coastal chl *a* trends (48), the western coast of South America was used to test the methods used in this paper. This region exhibited a strong positive trend in the Gregg et al. results, and the trend was similarly robust in (48).

Furthermore, our study covered a longer period (January 1998 – December 2007) than Gregg et al. (January 1999 – December 2003). This longer period may have accentuated lower values in the time-series occurring near the end of the study period; an example of this effect is seen in the Ganges River time-series.

The effect of the longer time-series may also be apparent in Vantrepotte and Mélin (49), which updated Gregg et al.'s results for the 10-year SeaWiFS data set. In their results, the absence of trends is clearly noted for the Amazon, Orinoco, and Congo outflow regions, and decreasing trends in agreement with our results are clearly noted for the Po, Missisippi East, and Ganges outflow regions. A positive trend near the outflow region of Galveston Bay is near the Mississippi East region, but the scale of the results is too coarse to allow comparison. No trend is noted near the Pearl River, and positive trends are located near our Eel and Guadalquivir regions, but it is again difficult to determine if our study region is located within the positive trend regions of (49). The general agreement of our results with those of Vantrepotte and Mélin is an encouraging indication that the relatively simple methodology of our techniques yields scientifically valid information.

It should also be noted that Kahru and Mitchell (50) observed trends of increasing bloom magnitude in areas prone to eutrophication, which includes the outflow zones of large rivers such as the Mississippi. Increases in bloom magnitude in such regions are not necessarily in conflict with our results because they may occur over relatively short time periods compared to the long-term record. Larger blooms could also be induced by stronger peak seasonal hydrologic flow in the rivers, due to a more pronounced melt season or increased precipitation in the watershed.

Summary

In general, the outflow zones of the largest rivers, which were also the rivers least influenced by human activity, did not exhibit significant trends. Most of the other river outflow zones did exhibit observable, and in many cases significant, trends, which we believe are primarily due to reduction of the average mean discharge of the river. This is even true for the Mississippi River, where the time-series covered a period with much higher discharge near the beginning of the time-series than near the end. This diminishment in flow can be attributed to human activity, regional climate change, interannual variability, or all of these factors in concert. The outflow zone of the Pearl River of China is the most notable exception, exhibiting a notable positive trend, which is likely due to increased nutrient loading in this river.

Observations of river-influenced coastal regions utilizing remotely-sensed chl *a* essentially integrate the influences of variable climate-related factors. In addition to discharge volume and nutrient content, other factors may include cloud cover, winds, and local temperatures, all of which can influence phytoplankton concentrations. Coastal currents may also induce changes. However, by using mapped monthly mean data, these factors become included in the overall assessment. A more detailed analysis can utilize higher spatial and temporal resolution data, and data more directly related to water quality, which is a planned developmental goal for the Giovanni system.

This paper demonstrates that utilizing the long-term SeaWiFS chl *a* data set in conjunction with Giovanni and MS Excel® to perform time-series analyses is an efficient way to examine bio-optical trends in the coastal zone. While this study does not utilize *in situ* data, performing more detailed examination of the factors which are implicated in these trends would require additional information, such as nutrient concentrations, salinity, sea surface temperature, sediment concentration, and optical characterization. The use of Giovanni with current and future ocean remote sensing data products, in conjunction with site-specific monitoring efforts, would likely yield important insight into the factors which are most relevant to the trends described here and by other authors.

ACKNOWLEDGEMENT

We wish to acknowledge the support of Erin McMahon at the Goddard Earth Sciences Data and Information Services Center during summer 2008 under the Student Internship Program (SIP) administered by the Goddard Space Flight Center Office of Higher Education.

This paper also benefited greatly from the comments provided by three anonymous reviewers, to whom we express our appreciation.

REFERENCES

1 Strange E M, K D Fausch & A P Covich, 1998. Sustaining ecosystem services in human-dominated watersheds: Biohydrology and ecosystem processes in the South Platte River Basin. Environmental Management, 23(1): 39-54

2 Ye B, D Yang & D L Kane. 2003. Changes in Lena River streamflow hydrology: Human impacts versus natural variations. Water Resources Research, 39(7): 1200; doi: 10.1029/2003WR001991

3 Gergel S E, M G Turner J R Miller, J M Melack & E M Stanley, 2002. Landscape indicators of human impacts to riverine systems. Aquatic Science, 64: 118-128

4 Surian N, 1999. Channel changes due to river regulation: The case of the Piave River, Italy. Earth Surface Processes and Landforms, 24: 1135-1151

5 Calder I R, R L Hall, H G Bastable, H M Gunston, O Shela, A Chirwa & R Kafundu, 1995. The impact of land use change on water resources in sub-Sahara Africa: a modeling study of Lake Malawi. Journal of Hydrology,170: 123-135.

6 Tang Z, B A Engel, B C Pijanowski & K J Lim, 2005. Forecasting land use change and its environmental impact at a watershed scale. Journal of Environmental Management, 76: 35-45

7 Palmer M A, C A R Liermann, C Nilsson, M Flörke, J Aleamo, P S Lake & N Bond, 2008. Climate change and the world's river basins: anticipating management. Front Ecolo Environ, 6, doi:10.1890/060148

8 Jain S & U Lall. 2001. Floods in a changing climate: does the past represent the future? Water Resources Research, 37(12): 3193-3205

9 Rabalais N N, W J Wiseman, R E Turner, B K Sen Gupta & Q Dortch, 1996. Nutrient changes in the Mississippi River and system response on the adjacent continental shelf. Estuaries, 19(2B): 386-407

10 Ætebjerg G, J Carstensen, K Dahl, J Hansen, K Nygaard, B Rygg, K Sørensen, G Severinsen, S Casartelli, W Schrimpf, C Schiller, J N Druon & A Künitzer, 2001. Eutrophication in Europe's coastal waters. European Environmental Agency
http://www.eea.europa.eu/publications/topic_report_2001_7/page001.html
(last date accessed: 09.11.2009)

11 Eplee R, R A Barnes, F S Patt, G Meister & C R McClain, 2004. SeaWiFS lunar calibration methodology after six years on orbit. In: Earth Observing Systems IX. Edited by W. L. Barnes and J J Butler, (Proceedings of the SPIE, Volume 5542) 1-13

12 Gregg W, N Casey, & C McClain, 2005. Recent trends in global ocean chlorophyll. Geophysical Research Letters, Vol. 32, L03606, doi:10.1029/2004GL021808

13 Acker J & G G Leptoukh, 2007. Online analysis enhances use of NASA earth science data. EOS, Transactions of the American Geophysical Union, Vol. 88 (2), 14 & 17.

14 Acker, J G, G G Leptoukh, S Kempler, S Berrick, H Rui & S Shen, 2007. Application of NASA Giovanni to Coastal Zone Remote Sensing Research. Proceedings, 3rd EARSeL Workshop *Remote Sensing of the Coastal Zone,* 7-9 June 2007, Bolzano, Italy (EARSeL, Strasbourg, France);
http://www.earsel.org/SIG-CZ/3rd_CZ_workshop/publications/wscz2007-acker.pdf
(last date accessed: 09.11.2009)

15 Acker J G, G Leptoukh, S Shen, T Zhu & S Kempler, 2008. Remotely-sensed chlorophyll-a observations of the northern Red Sea indicate seasonal variability and influence of coastal reefs. Journal of Marine Systems, 69: 191-204

16 Acker J G, L Harding, G Leptoukh, T Zhu & S Shen, 2005. Remotely-sensed chlorophyll *a* at the Chesapeake Bay mouth is correlated with annual freshwater flow to Chesapeake Bay. Geophysical Research Letters., 32, L05601, doi:10.1029/2004GL021852

17 Shen S, G G Leptoukh, J G Acker, Z Yu & S J Kempler, 2008. Seasonal variations of chlorophyll *a* concentrations in the Northern South China Sea. IEEE Geoscience and Remote Sensing Letters, 5: 315-319

18 Zar J.H, 1976. Biostatistical Analysis, 3rd Ed. (Prentice-Hall) 662 pp.

19 Milliman J D & J P M Syvitski, 1992. Geomorphic/Tectonic Control of Sediment Discharge to the Ocean: The importance of Small Mountainous Rivers. The Journal of Geology, 100: 525-544

20 Nittrouer, C A & D J DeMaster, 1996. The Amazon shelf setting: tropical, energetic, and influenced by a large river. Continental Shelf Research, 16(5/6): 553-573

21 Eisma D, J Kalf & S J Van Der Gaast, 1978. Suspended matter in the Zaire estuary and the adjacent Atlantic Ocean. Netherlands Journal of Sea Research, 12(3/4): 382-406

22 Meade R H, 1994. Suspended sediments of the modern Amazon and Orinoco rivers. Quaternary International, 21: 29-39

23 Meade R H, F H Weibezahn, W M Lewis Jr. & D P Hernandez, 1990. Suspended sediment budget for the Orinoco River. In: The Orinoco River as an Ecosystem, edited by F Weibezahn, H Alvarez & W M Lewis, Jr. (Impresos Rubel, Caracas), 55-80

24 Meade R H, 1995. Setting: Geology, hydrology, sediments, and the engineering of the Mississippi River. In: Contaminants in the Mississippi River, 1987-1992, edited by Robert H Meade. US Geological Survey Circular 1133 (Reston, Virginia) http://pubs.water.usgs.gov/circ1133/ (last date accessed: 09.11.2009)

25 Mississippi River/Gulf of Mexico Watershed Nutrient Task Force, 2008. Gulf Hypoxia Action Plan 2008 for Reducing, Mitigating, and Controlling Hypoxia in the Northern Gulf of Mexico and Improving Water Quality in the Mississippi River Basin http://www.epa.gov/msbasin/pdf/ghap2008_update082608.pdf (last date accessed: 09.11.2009)

26 Brown W M & J R Ritter, 1971. Sediment transport and turbidity in the Eel River Basin, California, U.S. Geological Survey Water Supply Paper 1986, 70pp.

27 Islam M R, S F Begum, Y Yamaguchi & K Ogawa, 1999. The Ganges and Brahmaputra rivers in Bangladesh: basic denudation and sedimentation. Hydrological Processes, 13: 2907-2923

28 World Wildlife Fund, 2004. Rivers at Risk: Dams and the future of freshwater ecosystems. Report, World Wide Fund for Nature and World Resources Institute (WWF), 48 pp. http://assets.panda.org/downloads/riversatriskfullreport.pdf (last date accessed: 09.11.2009)

29 Braga G & S Gervasoni, 1989. Evolution of the Po River: Example of the Application of Historic Maps. In Historic Change of Large Alluvial Rivers: Western Europe, edited by G E Petts, H Moller, & A L Roux (John Wiley & Sons) pp. 113-126

30 Syvitski J P M & A J Kettner, 2007. On the flux of water and sediment into the Northern Adriatic Sea. Continental Shelf Research 27(3-4): 296-308

31 Freudenreich H, J Saba & W Landsman. ROBUST_LINEFIT, The IDL Astronomy User's Library (NASA Goddard Space Flight Center, Greenbelt, Maryland) http://idlastro.gsfc.nasa.gov/ftp/pro/robust/robust_linefit.pro (last date accessed: 09.11.2009)

32 Moulton T P & K M Wantzen, 2006. Conservation of tropical streams – special questions or conventional paradigms? Aquatic Conservation: Marine and Freshwater Ecosystems, 16: 659-663

33 Lohrenz S E, D G Redalje, W-J Cai, J Acker & M Dagg, 2008. A retrospective analysis of nutrients and phytoplankton productivity in the Mississippi River plume. Continental Shelf Research, 28: 1466-1475

34 Walker N D & N N Rabalais, 2006. Relationships among satellite chlorophyll a, river inputs, and hypoxia on the Louisiana continental shelf, Gulf of Mexico. Estuaries and Coasts, 29(6B): 1081-1093

35 Mississippi River/Gulf of Mexico Watershed Nutrient Task Force, 2008. Gulf Hypoxia Action Plan 2008 for Reducing, Mitigating, and Controlling Hypoxia in the Northern Gulf of Mexico and Improving Water Quality in the Mississippi River Basin (Environmental Protection Agency, Washington, DC) 64 pp. http://www.epa.gov/msbasin/pdf/ghap2008_update082608.pdf (last date accessed: 09.11.2009)

36 Rabalais N N, R E Turner J Dubravko, Q Dortsch & W J Wisman Jr, 1998. Characterization of hypoxia–topic 1 report for the integrated assessment on hypoxia. In: *Gulf of Mexico: NOAA Coastal Ocean Program Decision Analysis Series* No. 17, 187 pp. http://www.cop.noaa.gov/pubs/das/das15.pdf (last date accessed: 09.11.2009)

37 Rabalais N N, R E Turner, Q Dortch, D Justic, V J Bierman Jr & W J Wiseman Jr, 2002. Review. Nutrient-enhanced productivity in the northern Gulf of Mexico: past, present and future. Hydrobiologia, 475/476: 39-63

38 Justic D, N N Rabalais & R E Turner, 1997. Impacts of climate change on net productivity of coastal waters: Implications for carbon budget and hypoxia. Climate Research, 8: 225-237

39 Lu X X, S R Zhang, S P Xie & P K Ma, 2007. Rapid channel incision of the lower Pearl River (China) since the 1990s as a consequence of sediment depletion. Hydrology and Earth System Sciences, 11(6), 1897-1906

40 Pearl River Water Resources Committee, 2003. Sediment Report. http://www.pearlwater.gov.cn/index.jsp (in Chinese) (last date accessed: 09.11.2009)

41 Zhu Z L & D L Chen, 2002. Nitrogen fertilizer use in China – Contributions to food production, impacts on the environment and best management strategies. Nutrient Cycling in Agroecosystems, 63(2-3): 117-127

42 Wang G, Q Sun, R Fu, X H Huang, J Wu, Y F He, A Dobermann & C Witt, 2004. Site-Specific Nutrient Management in Intensive Irrigated Rice Systems of Zhejiang Province, China. In: Increasing Productivity of Intensive Rice Systems through Site-Specific Nutrient Management, edited by A Dobermann, C Witt, & D Dawe (Science Publishers Inc., Enfield NH, USA, and International Rice Research Institute (IRRI), Los Baños, Philippines), p. 243-264

43 Seto K C, C E Woodcock, X Huang, J Lus & R K Kaufman, 2002. Monitoring land-use change in the Pearl River Delta using Landsat TM. International Journal of Remote Sensing, 23(10): 1985-2004

44 Adel M M, 2001. Effect on water resources from upstream water diversion in the Ganges basin. Journal of Environmental Quality, 30: 356-368

45 Webster P R & J Jian, 2007. Changes in the Discharge of Major Rivers in the Ganges, the Brahmaputra and the Yangtze Rivers During the Next 100 years. Eos, Transactions of the American Geophysical Union, 88(52), Fall Meeting Supplement, Abstract GC44A-07 http://www.agu.org/meetings/fm07/fm07-sessions/fm07_GC44A.html (last date accessed: 09.11.2009)

46 Guzzetti F, M Cardinali, P Reichenback, F Cipolla, C Sebastiani, M Galli & P Salvati, 2004. Landslides triggered by the 23 November 2000 rainfall event in the Imperia Province, Wester Liguria, Italy. Engineering Geology, 73(3-4): 229-245

47 Boldrin A, L Langone, S Miserocchi, M Turchetto & F Acri, 2005. Po River plume on the Adriatic continental shelf: Dispersion and sedimentation of dissolved and suspended matter during different river discharge rates. Marine Geology, 222-223: 135-138

48 Acker J, W Gregg, G Leptoukh, S Kempler, G Feldman, C McClain, W Esaias & S Shen, 2006. Use of Giovanni with Ocean Color Time-Series Project Data for Trend Detection in the Coastal Zone. In: Proc. Ocean Optics XVIII, October 9-13, 2006 (Montreal, Canada) http://disc.sci.gsfc.nasa.gov/oceancolor/PDFs/OO060208.pdf (last date accessed: 09.11.2009)

49 Vantrepotte V & F Mélin, 2009. Temporal variability of 10-year global SeaWiFS time-series of phytoplankton chlorophyll a concentration. ICES Journal of Marine Science, 66, 1547–1556

50 Kahru M & B G Mitchell, 2008. Ocean color reveals increased blooms in various parts of the world. Eos, Trans. AGU, 89(18): 170